

## Vacuum Arc Deposited Mo Layers: Grain Size and Roughness

B. Straumal<sup>1,3</sup>, N. Vershinin<sup>2</sup>, V. Semenov<sup>1,3</sup>, V. Sursaeva<sup>3</sup> and W. Gust<sup>1</sup>

<sup>1</sup> Max-Planck-Institut für Metallforschung and Institut für Metallkunde,  
Seestr. 75, D-70174 Stuttgart, Germany

<sup>2</sup> SONG Ltd., P.O. Box 98, Chernogolovka, Moscow District, 142432 Russia

<sup>3</sup> Institute of Solid State Physics, Russian Academy of Sciences, Chernogolovka,  
Moscow District, 142432 Russia

**Keywords:** Vacuum Arc Deposition, Grain Size, Roughness, Microparticles, Molybdenum

**Abstract**—The vacuum arc deposition process does not include sputtering and allows to reach high deposition rates for materials with a low sputter yield (e.g. refractory metals which are widely used as diffusion barriers). The roughness and grain structure of Mo films produced with the aid of vacuum arc deposition on Cu, silica glass and NaCl substrates have been studied. Mo films have a dense, non-textured polycrystalline structure. The grain structure of the Mo microparticles incorporated into the growing film cannot be distinguished from the film grain structure. The roughness of the Mo films studied increases with increasing deposition current and time. It decreases with increasing distance from the cathode. The interrelation between grain structure and surface morphology is discussed.

### 1. Introduction

The mobility of atoms controls the formation of the microstructure during the deposition of thin films and coatings. Close to the thermal equilibrium, namely in the simple case of vapour deposition, the changes in the thin film morphology (so-called structure zones) are governed mainly by the substrate temperature  $T_s$  [1, 2]. In zone I ( $T_s < 0.3 T_m$  for metals, where  $T_m$  is the melting temperature) the microstructure is porous and consists of tapered crystallites separated by voided regions the thickness of which is of the order of a few hundred angstroms. In zone II ( $0.3 T_m < T_s < 0.45 T_m$ ) the film has no porosity and consists of columnar grains separated by well-defined grain boundaries (GBs) with a width of about 5Å. In zone III (above  $0.45 T_m$ ) the structure consists of equiaxed grains. Experimental estimations of the activation energy [1] and both analytical and computer models [3] allow to attribute these structure zones to the ballistic aggregation control (zone I), surface (zone II) or bulk diffusion control (zone III). Later more sophisticated (and more non-equilibrium) deposition methods, like ion-assisted evaporation or magnetron sputtering, were developed [4]. The adequate structure zone models (SZMs) were also created [5] which take into account the thermal-induced mobility of the atoms in the growing layer together with the mobility induced by the bombardment with high-energy (tens to hundreds eV) ions [6, 7].

Recently, the important influence of low-energy (several tens eV) ion bombardment on the grain growth in coatings is also revealed [8]. Vacuum arc deposition is known as an effective method for the deposition of hard and decorative thick coatings [9–11]. Recently it has been shown that the vacuum arc deposition allows to reach high deposition rates (about 15 nm/s) for metals with low sputter coefficients (Mo) [12]. Unfortunately, data about the surface morphology and grain structure of vacuum arc deposited coatings are practically absent. The vacuum arc process differs from other well-studied deposition methods because the arc burns in the vapour of the cathode metal itself and, therefore, no sputtering is included. Thus, the morphology and grain structure of vacuum arc deposited coatings should be studied in dependence on the deposition parameters, and attempts should be made to attribute them to the known structure zones.

## 2. Experimental

Mo coatings have been deposited onto polished Cu, silica glass and cleaved NaCl substrates in a vacuum arc apparatus described elsewhere [12]. The pumping system of the apparatus consists of a Balzers turbomolecular pump with a capacity of 1500  $\ell$ /s and two rotary pumps with a total capacity of 40  $\ell$ /s. The pressure during deposition is  $8 \times 10^{-4}$  Pa. The vacuum chamber has the form of a horizontal cylinder of 700 mm diameter and 500 mm length. At the end of this cylinder the vacuum arc apparatus with the magnetic system for spot stabilization and the Mo cathode are placed. The cathode of diameter  $D = 60$  mm was made from 99.95% Mo. It was prepared by high-vacuum electron-beam multiple melting in specially designed water-cooled copper moulds [13]. The facilities for magnetic filtering of the macroparticles were not used in this study. The Cu, silica glass and fresh cleaved NaCl substrates were placed in different distances  $L$  from the surface of the cathode ( $L = 50, 175, 300$  and  $425$  mm). The vacuum arc source voltage was constant  $U = 31$  V, and the discharge current was changed ( $I = 80, 100, 140$  and  $180$  A). The strength of the stabilizing magnetic field on the cathode surface was 60 to 70 Gs. No bias has been applied to the substrates. The coating time was changed ( $t = 5, 10, 20$  and  $40$  min). In order to avoid an overheating of the substrates the coating process was interrupted (in vacuum) every 2.5 min for 2.5 to 3 min.

Plan-view examination with the aid of transmission electron microscopy (TEM) was performed with a JEOL model 100 CX TEM/STEM on films deposited onto freshly cleaved NaCl substrates and then floated off onto Cu grids. A dark field TEM based technique was used for the grain size measurements [7, 14]. A dark field image is formed by deflecting the electron beam to (110) reflection. It visualizes the grains which contribute to the diffracted beam. The mean grain size  $\langle d \rangle$  was determined using the standard methods of quantitative metallography. More than 200 grains were counted for each sample. The  $\langle d \rangle$  values measured from the dark field images in different diffracted beams coincide within the experimental error. The optical micrographs were made with the aid of a Zeiss Axiophot microscope. The roughness  $R_A$  was measured with the aid of a Sloan Dektak II profilometer and determined using the standard software.  $R_A$  was determined on two length scales, namely  $R_{A1000}$  for 1000  $\mu\text{m}$  and  $R_{A50}$  for 50  $\mu\text{m}$ . For each sample studied,  $R_A$  was measured in the direction perpendicular to the direction of the plasma flow 5 times at the length scale of 1000  $\mu\text{m}$  and 20 to 30 times on the length scale of 50  $\mu\text{m}$ . The measurements on the length scale 50  $\mu\text{m}$  were made mainly between the large particles.

## 3. Results and Discussion

Figure 1 displays a typical microstructure of the Mo films studied with TEM. Figure 1a shows a plan view electron diffraction pattern for a vacuum arc deposited Mo film. It indicates that the film contains randomly oriented microcrystals. The dark and bright field micrographs for the same film are shown in Figs 1b and c, respectively. The micrographs indicate random oriented non-clustered grain structure with  $\langle d \rangle = 15 \pm 4$  nm. There is no evidence of voids or porosity in the GBs or in the

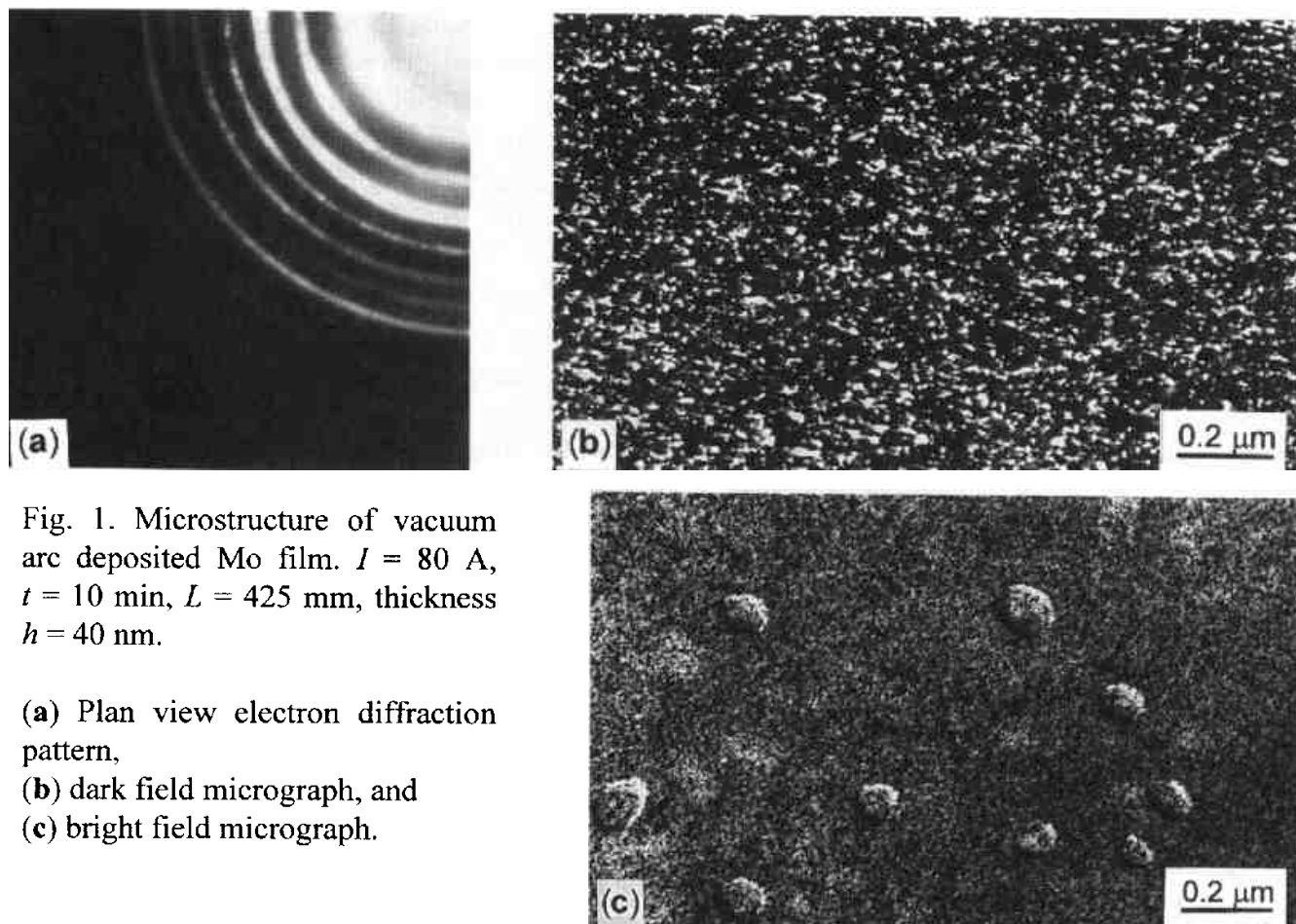


Fig. 1. Microstructure of vacuum arc deposited Mo film.  $I = 80$  A,  $t = 10$  min,  $L = 425$  mm, thickness  $h = 40$  nm.

- (a) Plan view electron diffraction pattern,  
 (b) dark field micrograph, and  
 (c) bright field micrograph.

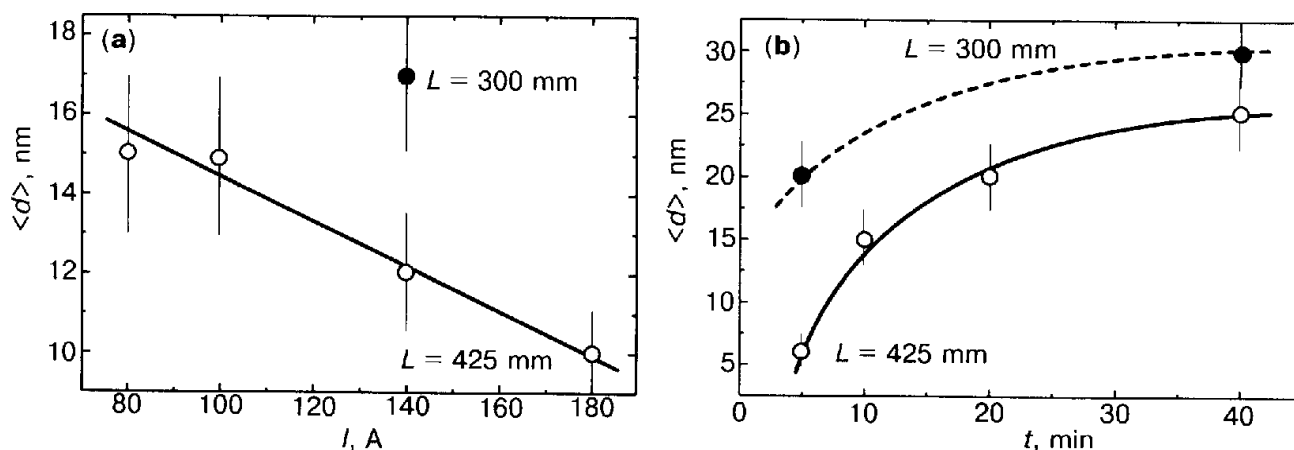


Fig. 2. Dependencies of the mean grain size  $\langle d \rangle$  (a) on the discharge current  $I$  for  $t = 10$  min and (b) on the deposition time  $t$  for  $I = 100$  A.

bulk. Such a microstructure is characteristic for the zone II of SZM (film growth controlled by surface diffusion) [1-3, 5-7]. An important feature of vacuum arc deposition is the formation of microparticles which fly to the substrate together with ions [15, 16]. Such particles can be seen in Fig. 1c. The grain size in the coating containing particles is the same as in the smooth region. On the plan TEM view all grains are seen which are present in the film. Obviously, the microparticles are still liquid as they stick to the coating, and grains from the underlying layer grow through these solidifying droplets. Therefore, the grain structure of microparticles after their solidification is incorporated into the overall grain structure of the growing coating.

The TEM measurements were possible only on Mo layers which are thin enough (high  $L$  or low  $I$  values). The  $\langle d \rangle$  values for these films change in a rather narrow interval of 10–100 nm. Figure 2 displays the dependencies of  $\langle d \rangle$  on the discharge current  $I$  and deposition time  $t$ . The values of  $\langle d \rangle$  for  $L = 300$  mm lie above the corresponding values for  $L = 425$  mm. In other words,  $\langle d \rangle$  decreases with increasing distance from the cathode.  $\langle d \rangle$  decreases slightly with increasing  $I$  (Fig. 2a). With increasing  $I$  the amount of the material supported to the substrate also increases. It facilitates the growth of nuclei at the early stages of the film growth and, therefore, leads to diminishing of  $\langle d \rangle$ . On the other hand, the increase of  $\langle d \rangle$  with increasing  $t$  (Fig. 2b) is an indication of grain growth during the deposition. This behaviour can be compared with the grain growth in Cu coatings exposed to the bombardment by low-energy ions [8].

Numerous theoretical and experimental studies show that the roughness of growing coatings depends strongly on the deposition process and can be described with the aid of fractal models [17]. Therefore, the roughness depends principally on the length of the measurement path and increases with increasing length scale [17, 18]. It has been recently shown that the morphology, mean size and distribution of the microparticles in Mo coatings produced with the aid of vacuum arc deposition depend strongly on  $L$ ,  $I$  and  $t$  [19]. The microparticles can influence drastically the roughness. Therefore, the roughness was measured on two length scales for each sample studied, namely 1000 and 50  $\mu\text{m}$ . The measurements on the 1000  $\mu\text{m}$  scale should characterize the overall roughness of the sample including the microparticles. The positions for the measurements on the 50  $\mu\text{m}$  length scale were chosen mostly between the large particles. These data describe the roughness of the coating formed due to the condensation of ions without the influence of the particles, at least at low coating times  $t$  when the area coated by particles is low and the overlapping of the particles is negligible.

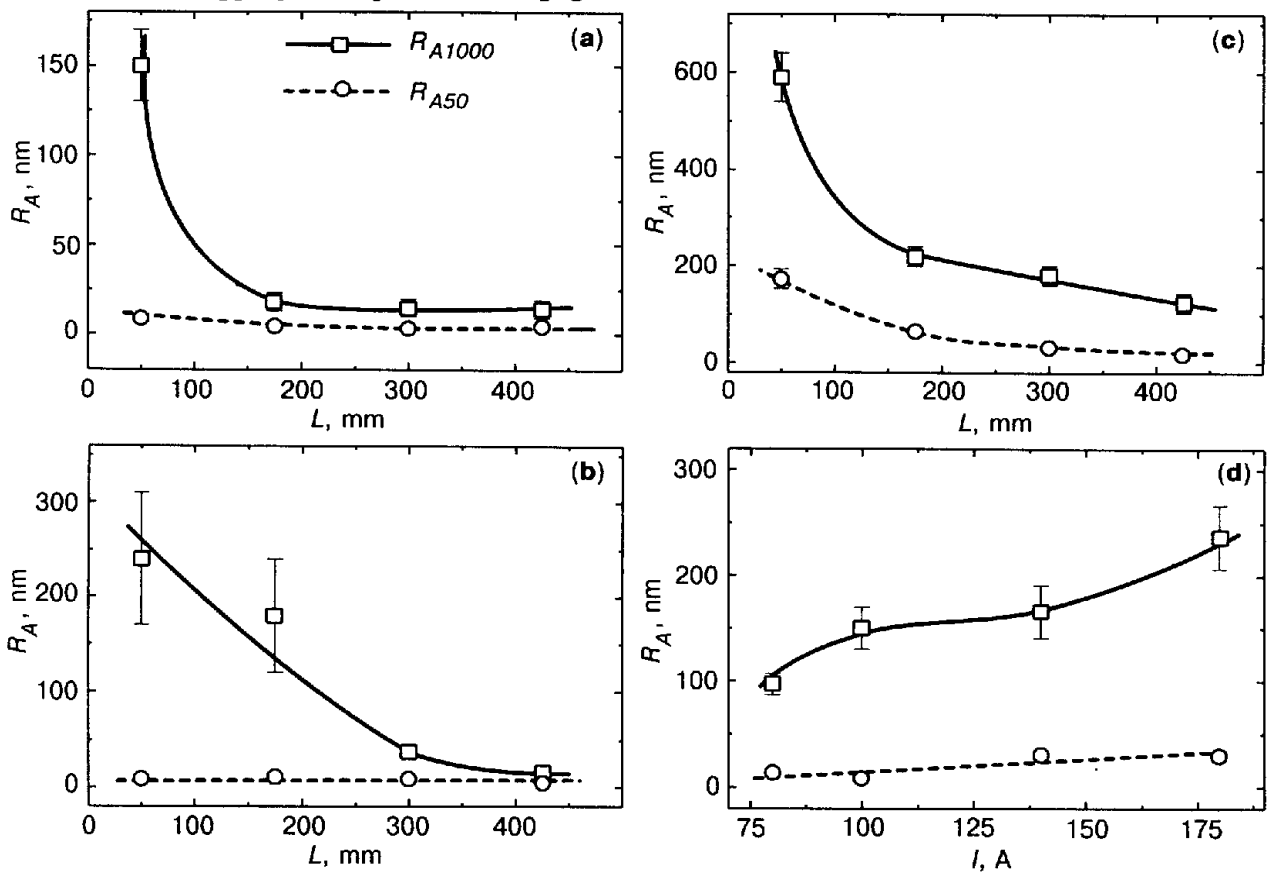


Fig. 3. Dependencies of the roughness values  $R_{A1000}$  and  $R_{A50}$  on the distance  $L$  and discharge current  $I$  for Mo films on Cu substrates. (a)  $\theta = 0^\circ$ ,  $I = 100$  A,  $t = 5$  min, (b)  $\theta = 90^\circ$ ,  $I = 100$  A,  $t = 5$  min, (c)  $\theta = 0^\circ$ ,  $I = 180$  A,  $t = 40$  min, and (d)  $\theta = 0^\circ$ ,  $L = 50$  mm,  $t = 5$  min.



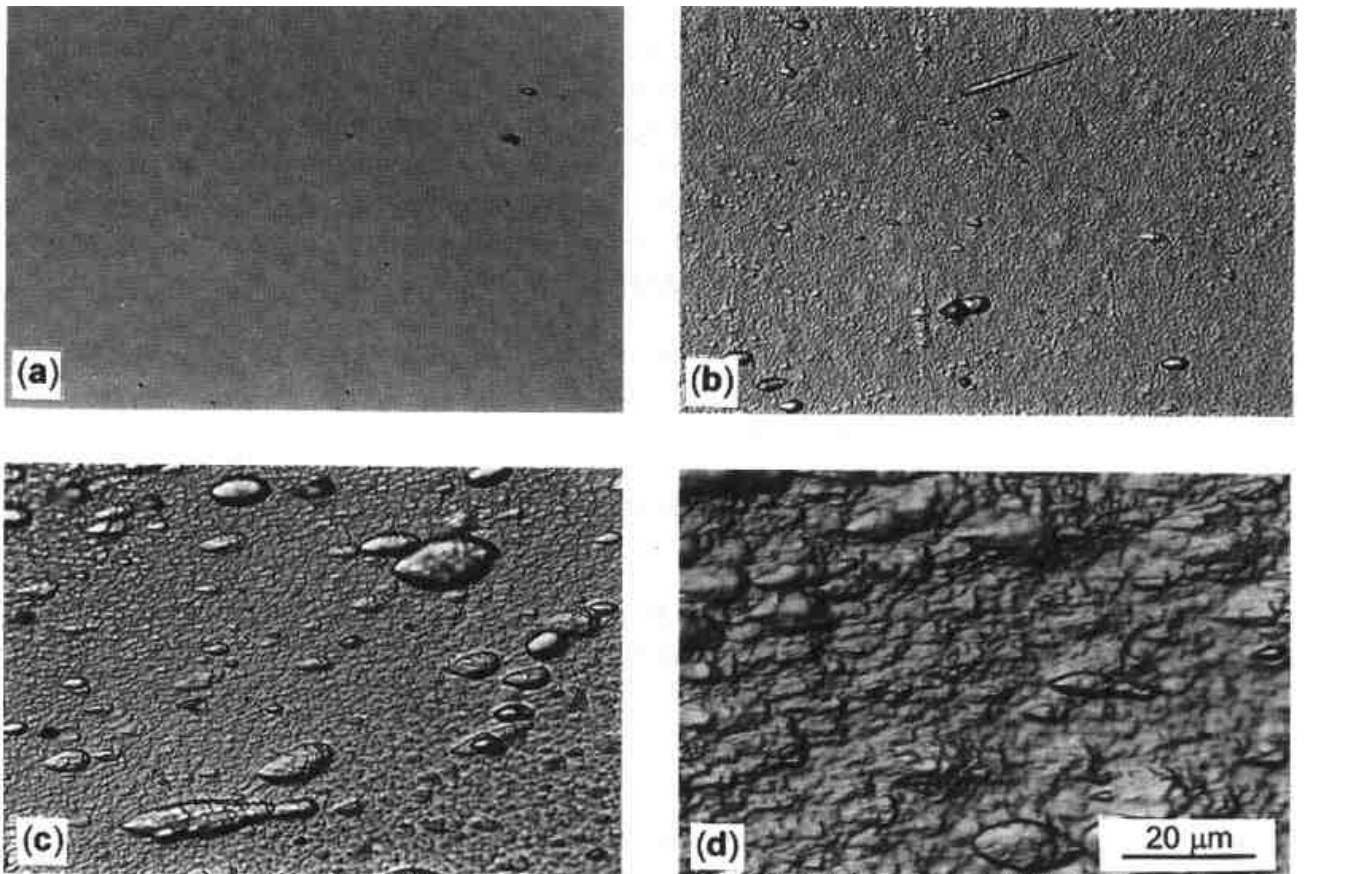


Fig. 4. The optical micrographs of the microstructure of Mo coatings on silica glass for  $\theta = 0^\circ$ . (a)  $I = 100$  A,  $L = 300$  mm,  $t = 5$  min, (b)  $I = 100$  A,  $L = 50$  mm,  $t = 5$  min, (c)  $I = 180$  A,  $L = 50$  mm,  $t = 5$  min, and (d)  $I = 100$  A,  $L = 50$  mm,  $t = 40$  min.

In Fig. 3 the dependencies of  $R_{A1000}$  and  $R_{A50}$  on the distance  $L$  are shown for different coating conditions. For a low deposition time (Figs 3a and b) a bi-modal roughness is present: individual particles can be clearly determined on the rather smooth background (see also the micrographs in Figs 4a and b). It can be supposed that the roughness of the coating between the microparticles is controlled mainly by the ion bombardment. The roughness of the background  $R_{A50}$  measured between the microparticles practically does not depend on  $L$  (Figs 3a and b) and is below 10 nm (this value is comparable with the roughness of ion-bombarded surfaces [18]). It is true both for substrates positioned parallel ( $\theta = 0^\circ$ , Fig. 3a) and perpendicular ( $\theta = 90^\circ$ , Fig. 3b) to the direction of the plasma flow. The measurements on the hillside of the extra large particles gave  $R_A$  values comparable with the  $R_A$  values at the 50  $\mu\text{m}$  scale on a flat surface. The values of  $R_{A50}$  coincide with the grain size measured by TEM (Figs 1 and 2). It can be, therefore, concluded that  $R_{A50}$  is defined by smooth circular caps between GBs which correspond to the steady state solution for the zone II (surface diffusion controlled film growth) [3].

The  $R_{A1000}$  values for  $\theta = 0^\circ$  are always higher than for  $\theta = 90^\circ$ . At the same time, the mean area of the individual particles for  $\theta = 0^\circ$  is lower than for  $\theta = 90^\circ$  [19]. Therefore, the particles on the substrates positioned parallel to the plasma flow are more flat than on the substrates positioned perpendicular to the plasma flow.  $R_{A1000}$  decreases with increasing  $L$  both for  $\theta = 0^\circ$  and  $\theta = 90^\circ$ . It correlates with a decrease of the number and size of the microparticles with increasing  $L$  [19]. With increasing deposition time the roughness increases, namely both  $R_{A1000}$  and  $R_{A50}$  (Fig. 3c). It is similar to the behaviour of the roughness of ion-eroded surfaces which also usually increases with

bombardment time [15, 20]. At high coating times not only  $R_{A1000}$  but also  $R_{A50}$  decreases with increasing  $L$ . It can be explained by the increase of the particle number with increasing  $t$  and by an overlapping of the particles (compare also the micrographs in Figs 4b and d). At low  $t$ , the increase of the discharge current  $I$  leads to an increase of  $R_{A1000}$  but does not influence  $R_{A50}$  (Fig. 3d). The behaviour of  $R_{A1000}$  can be explained by the increase of both the number and size of the microparticles with increasing  $I$  [19]. On the other hand, at  $t = 5$  min the particles practically do not overlap for any  $I$  values studied (compare Figs 4b and c). Therefore, the  $R_{A50}$  value does not exceed 30 nm and is not affected by a change of the discharge current.

The microstructure of the Mo coatings studied can be attributed to the zone II of SZM. In terms of a temperature-induced mobility it corresponds to the condition  $0.3 T_m < T_s < 0.45 T_m$ , though actually  $T_s < 0.08 T_m$ . Therefore, the bombardment with Mo ions with energy about 120–180 eV [21] during the vacuum arc deposition influences the film structure very strongly. It makes the vacuum arc deposition extremely attractive for different applications.

### Acknowledgements

The authors are grateful to Prof. Glebovsky and Prof. Shvindlerman for fruitful discussions. One of us (V.Semenov) wish to thank the Alexander von Humboldt Foundation for the financial support of his stay in Stuttgart. The financial support of the INTAS programme under grant 93-1451 is also acknowledged.

### References

- [1] B. A. Movchan, A. V. Demchishin, *Phys. Met. Metallogr.* **28**(4), 83 (1969).
- [2] J. A. Thornton, *J. Vac. Sci. Technol.* **11**, 666 (1974).
- [3] D. J. Srolovitz, A. Mazor, B. G. Bukiet, *J. Vac. Sci. Technol. A* **6**, 2371 (1988).
- [4] R. F. Bunshah (ed.), *Handbook of Deposition Technologies for Films and Coatings*, Noyes Publications, Park Ridge, NJ (1994).
- [5] R. Messier, A. P. Giri, R. A. Roy, *J. Vac. Sci. Technol. A* **2**, 500 (1984).
- [6] L. Li, W. B. Nowak, *J. Vac. Sci. Technol. A* **12**, 1587 (1994).
- [7] H. Kherandish, J. S. Colligon, J.-K. Kim, *J. Vac. Sci. Technol. A* **12**, 2723 (1994).
- [8] M. D. Naeem, S. M. Rosnagel, K. Rajan, *J. Vac. Sci. Technol. A* **13**, 209 (1995).
- [9] A.A. Snaper, US Patent 3 625 848 (1971), US Patent 3 836 451 (1974).
- [10] N. F. Vershinin, A. M. Dorodnov, A. N. Kuznetsov, USSR Patent 1 292 552 (1985).
- [11] L.P. Sablev, US Patent 3 783 231 (1974), US Patent 3 793 179 (1974).
- [12] N. F. Vershinin, B. B. Straumal, W. Gust, *J. Vac. Sci. Technol.*, to be published.
- [13] V. G. Glebovsky, B. M. Shipilevsky, I. V. Kapchenko, V. V. Kyreiko, *J. Alloys & Compounds*, **184**, 297 (1992).
- [14] V. G. Sursaeva, *Proc. MRS* **343**, 71 (1994).
- [15] J. Vysocil, J. Musil, *J. Vac. Sci. Technol. A* **10**, 1740 (1992).
- [16] A. Anders, S. Anders, I. G. Brown, M. R. Dickinson, R. A. MacGill, *J. Vac. Sci. Technol. B* **12**, 815 (1994).
- [17] J. Krim, I. Heyvaert, C. van Haesendonck, Y. Bruynseraede, *Phys. Rev. Lett.* **70**, 57 (1993).
- [18] G. S. Bales, R. Bruinsma, E. A. Eklund, R. P. Karunasiri, J. Rudnick, A. Zangwill, *Science* **249**, 264 (1990).
- [19] B. B. Straumal, W. Gust, N. F. Vershinin, V. G. Glebovsky, H. Brongersma, R. Faulkner, *Nucl. Instr. B*, to be published.
- [20] M. P. Sea, C. Lea, *Thin Solid Films* **81**, 257 (1981).
- [21] W. D. Dewis, H. C. Miller, *J. Appl. Phys.* **40**, 2212 (1969).